J Sol-Gel Sci Technol (2010) 54:282–285
DOI 10.1007/s10971-010-2191-z

ORIGINAL PAPER

Synthesis of ZnO nanobundles via Sol–Gel route and application to glucose biosensor

Zao Yang · Zhizhen Ye · Binghui Zhao · Xiaolin Zong · Ping Wang

Received: 13 November 2009 / Accepted: 2 March 2010 / Published online: 19 March 2010

Abstract ZnO nanobundles were fabricated by Sol–Gel route. The as-prepared ZnO nanobundles were characterized by XRD, FE-SEM, TEM and PL. ZnO nanobundles structure are composed of many nanorods of about 80 nm in diameter and 0.6 μm in length. It showed weaker UV emission and stronger green emission. A glucose biosensor was constructed using these ZnO nanobundles as supporting materials for glucose oxidase (GO_X) loading by chitosan-assisted cross-linking technique. The biosensor exhibits a high affinity, high sensitivity, and fast response for glucose detection. These results demonstrate that zinc oxide nanostructures have potential applications in biosensors.

Keywords ZnO · Nanobundles · Sol–Gel · Glucose biosensor

1 Introduction

The study of one-dimensional semiconductor nanostructures has attracted much attention in recent years because of their fundament scientific interest as well as potential applications in nanoscale electronic and optoelectronic devices [1]. ZnO, a wide-bandgap semiconductor ($E_g = 3.37$ eV at 300 k) with a large exciton binding energy (60 meV), is a versatile multifunctional material. The interest in the preparation of one-dimensional (1D) ZnO nanostructures continued in the past few years because of their potential uses as active components in the fabrication of UV nanolasers [2], field emission devices [3], dye-sensitized solar cells [4], photodetectors [5], and electroluminescent devices [6]. The synthesis of one-dimensional (1D) nano ZnO semiconductor materials ranging from needles [7], rods [8], belts [9], tubes [10], and so on has attracted considerable research interest because of their great potential for fundamental studies of the roles of dimensionality and size in their physical properties as well as for applications of building blocks and interconnects in electronic and photonic devices [11].

On the other hand, ZnO is a biocompatible material with a high isoelectric point (IEP) of about 9.5, which make it suitable for absorption of proteins with low IEPs, as the protein immobilization is primarily driven by electrostatic interaction [12]. Moreover, ZnO nanostructures have unique advantages including the high specific surface area, nontoxicity, chemical stability, electrochemical activity, and high electron communication features. Hence, they are promising for biosensor applications.

In this article, we fabricate ZnO nanobundles by Sol–Gel route. The as-prepared ZnO nanobundles were characterized by XRD, FE-SEM, TEM and PL. ZnO nanobundles structure are composed of many packed nanorods of about 80 nm in diameter and 0.6 μm in length. It showed weaker UV emission and stronger green emission. A glucose biosensor was constructed using these ZnO nanobundles as supporting materials for glucose oxidase (GO_X) loading by chitosan-assisted cross-linking technique. The biosensor exhibits a high affinity, high sensitivity, and fast response for glucose detection. These results

Z. Yang (✉) · Z. Ye · B. Zhao
State Key Laboratory of Silicon Materials, Department of Materials Science and Engineering, Zhejiang University, 310027 Hangzhou, China
e-mail: yangzao888@tom.com

X. Zong · P. Wang
Biosensor National Special Laboratory, Key Laboratory of Biomedical Engineering of National Education Ministry, Department of Biomedical Engineering, Zhejiang University, 310027 Hangzhou, China

demonstrate that zinc oxide nanostructures have potential applications in biosensors.

2 Experimental

All the chemicals used in this study were of analytical grade and used without farther purification. Four chemicals were needed and they were analytically pure Zinc acetate (Zn $(CH_3COO)_2{\cdot}2H_2O$), citric acid ($C_6H_8O_7{\cdot}H_2O$), pure distilled water (H_2O) and absolute ethanol (CH_3CH_2OH). In a typical procedure, a solution of citric acid (0.128 M) in ethanol was added to Zn $(CH_3COO)_2$ solutions (3.2 M) in distilled water. After the addition was finished, the solution (PH value was equal to 6.1) was stirred at 355 K for 9 h to get the precursor. The precursor was calcined in a muffle furnace for 2 h at 683 K. Finally, the sample was obtained after cooling down at room temperature in air.

The morphologies of products were investigated by scanning electron microscopy (FE-SEM, HITACHI S-4800) and transmission electron microscopy (TEM JEM-2010). The X-ray diffraction (XRD) patterns were measured by Rigaku D/max—rA with Cu k_a radiation. Photoluminescence (PL) measurements were performed at room temperature by using a He–Cd laser (325 nm) as the excitation source.

For the fabrication of a glucose sensor, the glassy carbon (GC) electrodes was polished by 0.3 and 0.05 μm aluminum slurries and then was cleaned by dipping into 1:1(V/V) aqueous solution of HNO_3, deionized water and ethanol with the assistance of ultrasonication prior to the experiment. The as-prepared ZnO nanobundles were dispersed, in ethanol by ultrasonication for 1 h to 5×10^{-3} M suspension. Firstly, 5 μL of ZnO nanobundles suspension was dropped onto the surface of GC electrode and dried at room temperature. Secondly, 5 μL of GO_x solution with concentration of 1934 U (biologic active unit)/mL prepared in 0.01 M phosphate buffer solution (PH 7.4) was droped onto the surface of GC electrode modified by ZnO nanobundles. Finally, 5 μL of 0.5wt% CHIT (Chitosan) solution dissolved in acetic acid solution was dropped onto the surface of GO_x/ZnO nanobundles/GC electrode to avoid the leakage of the enzyme. The device was drived at 277 K overnight in a refrigerator, followed by washing step to remove the unimmobilized GO_x. The CHIT/GO_x/ZnO nanobundles/GC electrode was stored in PBS and kept at 277 K in a refrigerator when not in use.

3 Results and discussion

The X-ray diffraction pattern of the as-grown ZnO nanobundles is shown in Fig. 1. The diffraction peaks can be

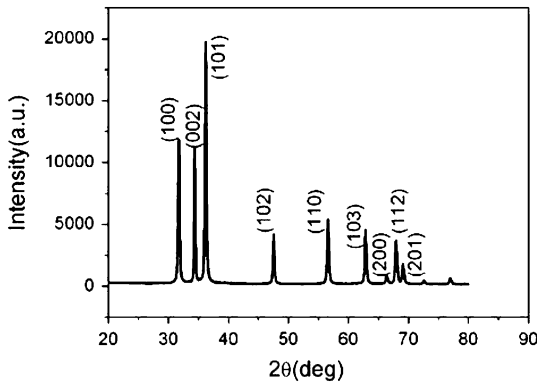

Fig. 1 XRD patterns of as-grown ZnO nanobundles

indexed as the wurtzite structure in the standard data (JCPDS, 36-1451). (ZnO belongs to the hexagonal space group, $P6_3mc$ (186); unit-cell parameters, averaged among the cited PDF cards: a = 3.249 Å, c = 5.206 Å). No other diffraction peaks were found.

To investigate the morphologies of the synthesized ZnO nanostructures, the morphology of the products was observed by FE-SEM. The typical FE-SEM images were shown in Fig. 2. It can be clearly seen that ZnO nanobundles are composed of many packed nanorods of about 80 nm in diameter and 0.6 μm in length. Parts of the nanorods tend to parallel-arrange tightly and show an obvious trend to attach to each other. The diameters of most nanorods are almost same throughout their length and all exhibited smooth and clean surfaces with a slight reduction in diameter at their tips. Due to its anisotropic nature, ZnO prefers to grow along the c axis.

To further obtain the structural information of the ZnO products, typical TEM are recorded as shown in Fig. 3. Figure 3 reveals the TEM image of the whole ZnO nanobundles shape. The result shows that ZnO nanorods have diameter in the range of 80 nm and length of 0.6 μm, which is similar to that shown in Fig. 2. It also shows that

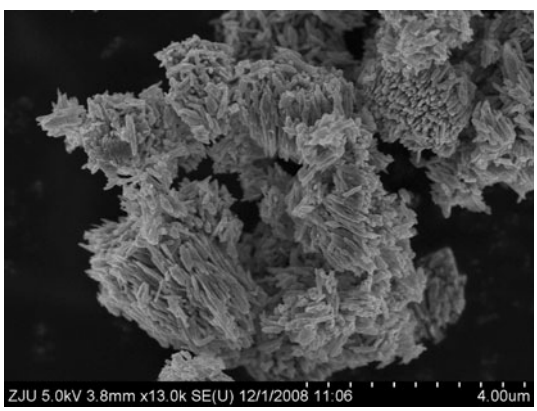

Fig. 2 FE-SEM images of the ZnO nanobundles

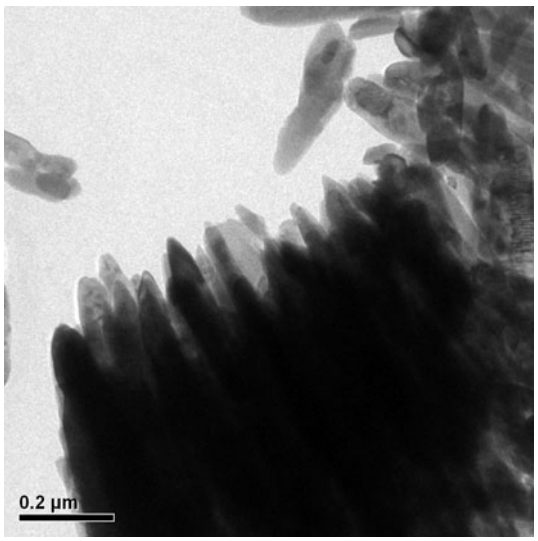

Fig. 3 TEM image of as-grown ZnO nanobundles

the ends of the nanorods have relatively smaller diameters compared with that of the middle parts. It is noteworthy that the ZnO nanobundles structures are sufficiently stable, which cannot be destroyed even after ultrasonication for a long time.

Photoluminescence (PL) spectrum of ZnO nanobundles at room temperature was measured and shown in Fig. 4. Both the UV emission and the green emission can be observed clearly. The UV emission is due to the near band-edge free exciton transition from the localized level below the conduction band to the valance band, namely, the recombination of free excitons through an exciton–exciton collision process. The peak around 512 nm is due to the green emission that is commonly referred to as deep-level and trapstate emission. The deep-level emission is mainly related to point defects, such as Zn interstitials and oxygen vacancies. Oxygen vacancies occur in three different charge states: the neutral oxygen vacancy (V_O^0), the singly ionized oxygen vacancy $(V_O^{\bullet})$, and the doubly ionized oxygen vacancy $(V_O^{\bullet\bullet})$ and only $(V_O^{\bullet})$ can act as the so-called luminescence centers [13]. The green emission is much stronger than the UV emission and the UV emission shift a little to 382 nm because of the small size of the ZnO nanostructures [14].

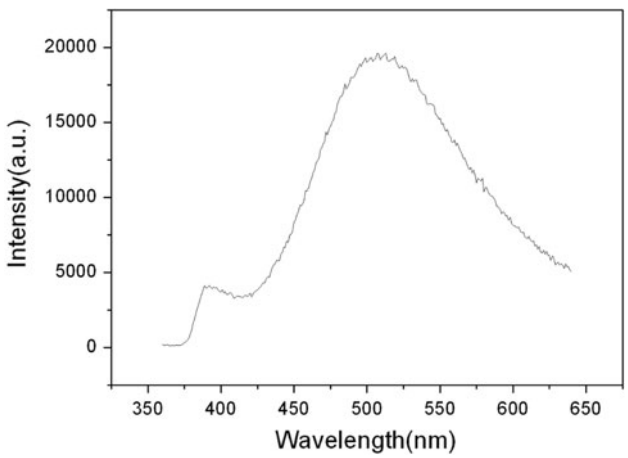

Fig. 4 PL spectrum of ZnO nanobundles at room temperature

The enzyme electrode was characterized by cyclic voltammetry between the potentials of −0.2 and 0.8 V, as shown in Fig. 5. 136.87 U/cm^2 GO_X per unit area of the ZnO-immobilize d GC electrode. In enzymatic glucose sensors, GOD is typically used as the biological enzyme to form the electrochemical transducer. In the presence of oxygen, GOD can catalyze the electro-oxidation of glucose. The following equations show the path and indicate the reaction mechanism for the determination of glucose:

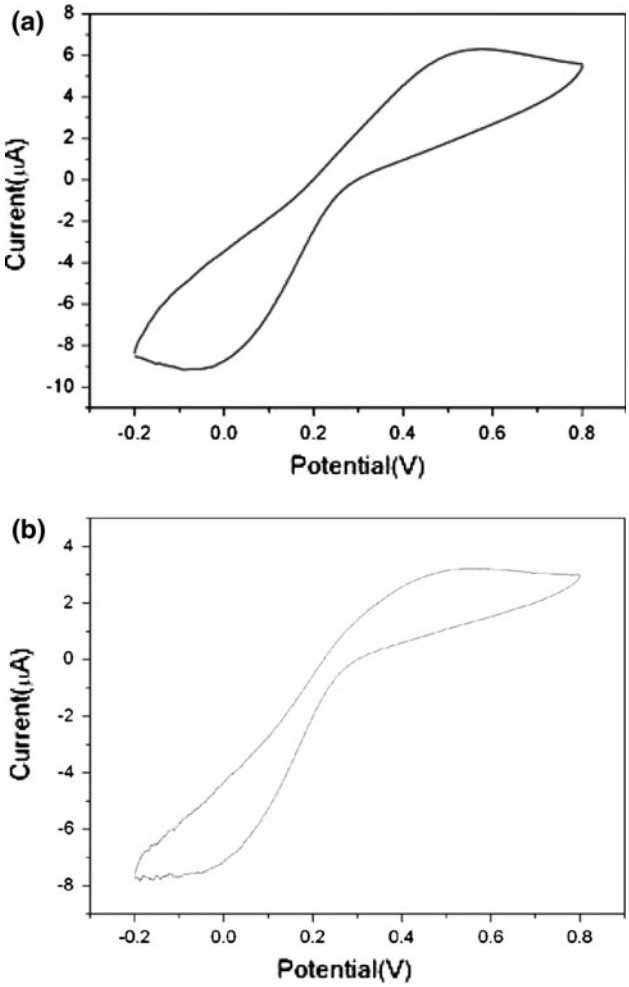

Fig. 5 **a** Cyclic voltammograms of the CHIT/GO_x/ZnO nanobundles/GC electrode. **b** Cyclic voltammograms of the CHIT/GO_x//GC electrode

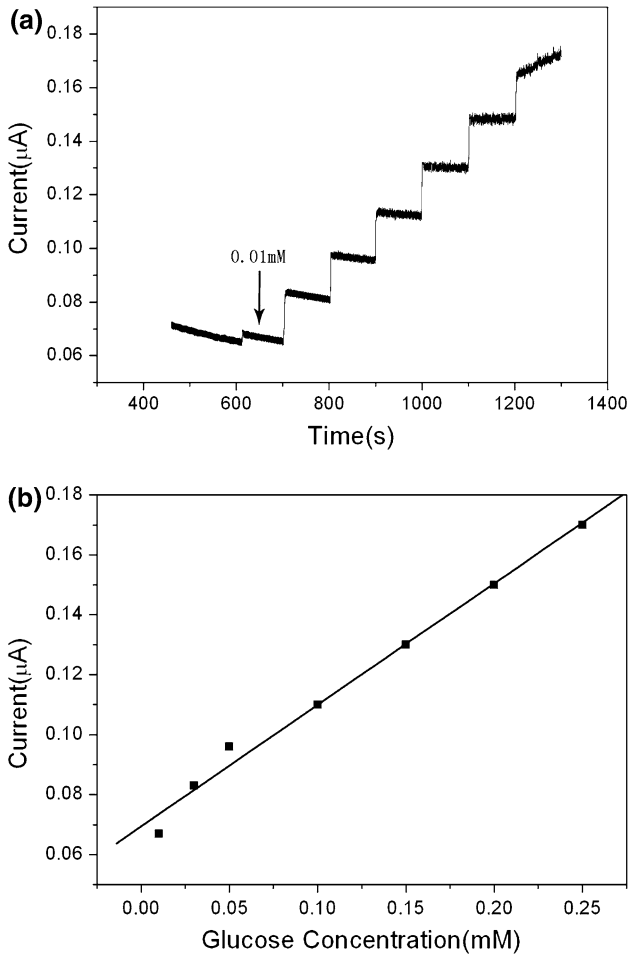

Fig. 6 **a** Amperometric responses of CHIT/GO_x/ZnO nanobundles/GC electrodes with the successive addition of 50 mM glucose to the 0.01 M, pH 7.4 PBS buffer under stirring. **b** Linear calibration curve of ZnO nanobundles/GO_x biosensor (0.01–0.25 mM)

$$\text{glucose} + O_2 \xrightarrow{\text{GOD}} \text{gluconic acid} + H_2O_2$$

As is shown in Fig. 5a, a pair of redox peaks with formal potential at −0.084 and 0.574 versus reference electrode can be obtained with CHIT/GO_x/ZnO nanobundles modified electrode which can be assigned to reversible redox reaction of potassium ferricyanide. Curve in stirred 0.01 M (pH 7.4) phosphate buffer solution in the presence of 1 mM potassium ferricyanide. In contrast, only a small pair of redox peaks can be observed at the CHIT/GO_x modified electrode. The nice electrochemical response can be obtained with the help of ZnO nanobundles, and the enzyme can exhibit fine electrocatalytic activity.

Figure 6a is a typical amperometric response of the glucose biosensor for successive of 0.05 M glucose in 0.01 M PBS buffer (pH 7.4) at an applied potential of 0.8 V under stirring. It can be seen from the plot that the biosensor shows a rapid and sensitive response to the change of glucose concentrations, indicating a good electrocatalytic property of CHIT/GO_x/ZnO nanobundles/GC electrode. The corresponding calibration curve (Solid Square) of the glucose biosensor is shown in Fig. 6b. The linear range of the calibration curve is from 0.01 to 0.25 mM (correction coefficient $R = 0.9948$) and a limit of detection (LOD) of 0.01 mM.

4 Conclusions

ZnO nanobundles were fabricated by Sol–Gel route. The as-prepared ZnO nanobundles structure is composed of many packed nanorods of about 80 nm in diameter and 0.6 μm in length. The as-prepared ZnO nanobundles showed weaker UV emission and stronger green emission. We have demonstrated a glucose biosensor based on our grown ZnO nanobundles. The results showed that the ZnO nanobundles formed an attractive matrix for GO_x immobilization, which exhibits a high affinity, high sensitivity, and fast response for glucose detection.

Acknowledgments This work was partly supported from "973" National Key Basic Research Program of China (Grant No. 2006CB 604906). Postdoctoral fund of Zhe Jiang province (2009-bsh-003).

References

1. Xia Y, Yang P, Sun Y, Wu Y, Mayers B, Gates B, Yin Y, Kim F, Yan H (2003) Adv Mater 15:353
2. Huang MH, Mao S, Feick H (2001) Science 292:1897
3. Wang WZ, Zeng BQ, Yang J, Poudel B, Huang JY, Naughton MJ, Ren ZF (2006) Adv Mater 18:3275
4. Law M, Greene LE, Johnson JC, Saykally R, Yang P (2005) Nat Mater 4:455
5. Law JBK, Thong JTL (2006) Appl Phys Lett 88:133114
6. Park WI, Yi GC (2004) Adv Mater 16:87
7. Ledwith D, Pillai SC, Watson GW, Kelly JM (2004) Chem Commun 2294
8. Yang Z, Liu QH, Yang L (2007) Mater Res Bull 42:221
9. Pan ZW, Dai ZR, Wang ZL (2001) Science 291:1947
10. Vayssieres L, Keis K, Hagfeldt A, Lindquist SE (2001) Chem Mater 13:4395–4398
11. Dai Y, Zhang Y, Wang ZL (2003) Solid State Commun 126:629–632
12. Liu ZM, Liu YL, Yang HF, Yang Y, Shen GL, Yu RQ (2005) Electroanalysis 17:1065
13. Kang HS, Kang JS, Kim JW, Lee SY (2004) J Appl Phys 95:1246
14. Wang XD, Ding Y, Summers CJ, Wang ZL (2004) J Phys Chem B 108:8773–8777